Numerical treatment of seismic accelerograms and of inelastic seismic structural responses using harmonic wavelets

P.D. Spanos[1], A. Giaralis[2], N.P. Politis[3], J. Roessett[4]

[1]L. B. Ryon Chair in Engineering, Rice University, Houston, Texas

[2]Ph.D. Candidate, Department of Civil Engineering, Rice University, Houston, Texas

[3]Floating Systems Engineer, BP America Inc.

[4]Cain Chair in Civil Engineering, Texas A&M University, College station, Texas

Abstract

The harmonic wavelet transform is employed to analyze various kinds of nonstationary signals common in aseismic design. The effectiveness of the harmonic wavelets for capturing the temporal evolution of the frequency content of strong ground motions is demonstrated. In this regard, a detailed study of important earthquake accelerograms is undertaken and smooth joint time- frequency spectra are provided for two near- field and two far- field records; inherent in this analysis is the concept of the mean instantaneous frequency. Further, as a paradigm of usefulness for aseismic structural purposes, a similar analysis is conducted for the response of a 20-story steel frame benchmark building considering as the excitation one of the four accelerograms scaled by appropriate factors to simulate undamaged and severely damaged conditions for the structure. The resulting joint time- frequency representation of the response time histories captures the influence of nonlinearity on the variation of the effective natural frequencies of a structural system during the evolution of a seismic event. In this context, the potential of the harmonic wavelet transform as a detection tool for global structural damage is explored in conjunction with the concept of monitoring the mean instantaneous frequency of records of critical structural responses.

1. Introduction

Seismic signals are inherently nonstationary as their intensity and frequency content evolve with time. Earthquake accelerograms decay in time, after a short initial period of growth, and exhibit a time-varying frequency composition due to the dispersion of the propagating seismic waves. Since the response of a structural system to a strong ground motion is primarily a resonance problem, capturing the evolution of the frequencies present in a seismic accelerogram facilitates the assessment of its damage potential to constructed facilities. Furthermore, the time histories associated with certain structural response quantities, such as floor displacements and inter-story drifts of a building subject to seismic excitation, can also be processed as nonstationary signals whose evolving frequency contents not only reflect, obviously, some characteristics of the input excitation but also carry valuable information about the possible level of global structural damage caused by the motion of the ground. Such signals call for a joint time-frequency analysis; for it is clear that their time- dependent frequency content cannot be adequately represented by the ordinary Fourier analysis which provides only the average spectral decomposition of a signal.

During recent decades the wavelet transform has become a potent analysis tool in signal processing that can be used to yield a well defined time-frequency representation of a deterministic signal; see for instance Burrus et al. (1997) and Mallat (1998). In most cases, it is advantageous compared to traditional time- frequency analysis methods such as the windowed or short- time Fourier transform (STFT), and the Wigner- Ville distribution (WVD) (e.g. Newland, 1997). STFT involves truncating the signal in time using possibly overlapping window functions of a chosen width T to obtain piecewise

stationary signals of constant duration T. Then, Fourier analysis is performed to each of these pieces of the initial signal resulting in Fourier coefficients that feature the same frequency bandwidth of approximately 1/T, due to the uncertainty principle (Cohen, 1995). This constitutes a non- adaptive analysis procedure with significant time-frequency resolution limitations. Once the window function is chosen, the frequency and time resolution are fixed for all frequency bands and all times. To assume stationarity, the window is supposed to be narrow, which results in poor frequency resolution. If the width of the window is increased, the frequency resolution improves but the time resolution becomes poor and the condition of stationarity may be violated.

The Wigner- Ville method aims to circumvent some of the shortcomings of STFT and is based on the concept that a time- dependent spectrum at time t can be defined as the Fourier transform of an instantaneous correlation function $R(\tau, t)$, which corresponds to the standard correlation function $R(\tau)$ with time lag τ centered at time t (Cohen, 1995; Newland, 1997; Spanos and Failla, 2004). Clearly, WVD utilizes the non decaying in time harmonic sinusoids and thus the variable τ must be integrated over an infinite range to compute the Fourier coefficients of $R(\tau, t)$, yielding a spectrum that cannot reflect the actual local behavior of the signal at time t. In this respect, the WVD poses the same fundamental problem that limits the STFT. Furthermore, the WVD lacks, to a certain degree, physical meaning since in several cases it yields negative values for the spectrum with obvious physical interpretation problems (Cohen, 1995).

The wavelet transform overcomes the aforementioned difficulties. It provides a time- frequency representation of a signal based on a double series of basis functions called “wavelets” (small waves). Wavelets have an oscillatory wave-like form with

certain frequency content and localized energy in time. They are generated by scaling and shifting a single "mother wavelet" function. Scaling allows the time duration of the wavelet to be adjusted according to the local frequency content of the signal, contrary to the harmonic sinusoids used in all Fourier- based techniques that have infinite support in time. Thus, small or large scales can be selected to capture high- or low- frequency components, respectively, with a significant reduction of the requisite computational effort as compared to the STFT.

A plethora of wavelet functions capable of generating meaningful analyzing basis has been developed to best suit several problems in science and engineering related to transient, time-variant, or non-stationary phenomena. This fact endows the method with flexibility which constitutes another reason for its popularity among many researchers. In a recent review article by Spanos and Failla (2005), an extensive reference list is provided citing numerous publications incorporating the wavelet analysis for random field simulation, system identification, damage detection and other structural engineering and vibration applications. Additionally, Zhou and Adeli (2003a, 2003b), considered the Mexican hat wavelets to analyze earthquake accelerograms in time-frequency domain, while Qang and Deng (1999), Hou et. al (2000), and Spanos et. al (2006) used spatial wavelets to detect damage in structural members.

The family of generalized harmonic wavelets introduced by Newland (1994a, 1994b), possesses the appealing property of non- overlapping Fourier transforms which renders the corresponding harmonic wavelet transform an exceptional tool in cases where enhanced resolution in the frequency domain is important. To enhance the time resolution as well, the filtered harmonic wavelets were proposed later by the same author (Newland,

1999). The harmonic wavelet transform has been used in geotechnical earthquake engineering in conjunction with the spectral analysis of surface waves to estimate the shear wave velocity of soil layers (Kim and Park, 2002), as well as in soil dynamics for analyzing transient vibration data from centrifuge model experiments to study liquefaction of saturated sands (Newland and Butler, 2000; Haigh et al., 2002).

The present article extends earlier efforts made (Spanos et al., 2005), in using filtered harmonic wavelets for capturing local effects on various nonstationary signals frequently encountered in earthquake and structural engineering. Previous works by Haigh et al. (2002) and Spanos et al. (2005), have considered the analysis of recorded earthquake accelerograms associated with major seismic events via the harmonic wavelet transform. Herein, a more systematic study of strong ground motions is undertaken and smooth joint time- frequency spectra are provided for important near-field (two) and far- field (two) recorded seismic events (Spencer et al., 1999; Ohtori et al., 2004), featuring the concept of the mean instantaneous frequency (Boashash, 1992a; Boashash, 1992b; Cohen, 1995).

Furthermore, the joint time-frequency harmonic wavelet analysis is used to complement early works such as that of Roesset (1986), to capture the influence of nonlinearity on the variation of the effective natural frequencies of a structural system during the evolution of a seismic event. For this purpose, nonlinear step-by-step in time analysis is performed for a benchmark 20- story steel frame building described in Spencer et al. (1999), and Ohtori et al. (2004), excited by one of the above mentioned strong ground motions scaled by various factors. Appropriate numerical results for certain of the response time histories analyzed by means of the harmonic wavelet

transform are presented. They pertain to undamaged and severely damaged structural conditions, and demonstrate that the mean instantaneous frequency of a signal can be used as a detection tool for global structural damage.

2. Harmonic wavelets and Mean instantaneous frequency of signals

Consider a function $f(t)$ in the time domain satisfying the finite energy condition

$$\int_{-\infty}^{\infty} |f(t)|^2 \, dt < \infty . \tag{1}$$

The classic *Fourier transform* decomposes the function $f(t)$ by projecting it onto the basis of sinusoidal functions with varying frequencies. For each frequency value, a *Fourier coefficient* is assigned and the two-dimensional (2-D) Fourier amplitude spectrum of $f(t)$ is obtained by plotting those coefficients versus frequency. Note that sinusoids are represented by delta functions in the frequency domain, yielding excellent frequency resolution but have no strong temporal localization features.

The *Wavelet transform* uses a basis of functions generated by appropriately dilating and then translating in time a single *mother wavelet function*. Generally, they are oscillatory functions of zero mean and absolutely integrable and square integrable (i.e. of finite energy in L_1 and L_2 norm). Dilation is achieved by modifying the *scale parameter* α which controls the frequency content of the wavelet function, while translation in time is accomplished by altering the *time parameter b*. Thus, the Wavelet transform provides a joint time-frequency representation of $f(t)$ by assigning a number of *wavelet coefficients* at different scales, extending the traditional concept of frequency, and time positions. The

most general form of the continuous wavelet transform (CWT) of $f(t)$ is given by the equation

$$w(a,b) = \frac{1}{\sqrt{a}} \int_{-\infty}^{\infty} f(t) \psi^* \left(\frac{t-b}{a} \right) dt , \quad (2)$$

where the function $\psi(t)$ denotes the mother wavelet, and w(a,b) is the wavelet coefficient at scale a and time position b. The symbol (*) denotes complex conjugation. Typically, such an analysis results in a 3-D spectrum having the wavelet coefficients plotted versus time and scale. However, caution should be exercised on defining time, and distinguishing scale from frequency and the relationship between them which depends on the wavelets used and their form. For symmetric wavelets in the time domain, time is usually defined as the center of their time window and the same holds respectively for symmetric wavelets in the frequency domain. Otherwise, the mean time and the mean frequency of the wavelet serve for time and frequency in the 3-D spectral map.

Harmonic wavelets are specifically defined to have a *band limited spectrum*. In general, two indices (m, n), are used to define their finite support in the frequency domain and thus to control their frequency content. Two different kinds of time-frequency representation have been introduced by Newland (1994a, 1994b), in conjunction with the *harmonic wavelet transform (HWT),* and the treatment of deterministic signals; the *dyadic* and the *generalized harmonic wavelet schemes*, the first being a special case of the second for $m= 2^{\alpha}$ and $n= 2^{\alpha+1}$. Later, the *filtered harmonic wavelet scheme* was presented by the same author to enhance the time resolution of the generalized scheme (Newland, 1999; Spanos et al., 2005). Previous work such as in Spanos et al. (2005), suggests that the filtered harmonic wavelet scheme improves significantly the time

resolution of the wavelet transform, and does compensate for its increased computational cost by being capable of adequately capturing the change in the frequency content of seismic signals. Herein, the last scheme is briefly reviewed as it is exclusively used in the ensuing analyses.

The filtered harmonic wavelets scheme incorporates a Hanning window function in the frequency domain to improve the time localization capabilities of the HWT in the wavelet mean square map for a given frequency resolution (Newland, 1999; Spanos et al., 2005). The wavelet function of scale (m, n) and position (k) in the frequency domain takes the form

$$\hat{\Psi}_{(m,n),k}(\omega)=\begin{cases}\dfrac{1}{(n-m)2\pi}\left(1-\cos\left(\dfrac{\omega-m2\pi}{n-m}\right)\right), & m2\pi\le\omega\le n2\pi\\ 0, \quad \text{elsewhere}\end{cases}, \tag{3}$$

where m and n are assumed to be positive, not necessarily integer numbers. By application of the inverse Fourier transform in Eq. (3) one obtains its complex- valued time domain counterpart (Spanos et al., 2005), with magnitude

$$\left|\psi_{(m,n),k}(t)\right|=\frac{\sin\pi\left(t-\dfrac{k}{n-m}\right)(n-m)}{\pi\left(t-\dfrac{k}{n-m}\right)\left(\left(t-\dfrac{k}{n-m}\right)^2(n-m)^2-1\right)}, \tag{4}$$

and phase

$$\varphi_{(m,n),k}(t)=\pi\left(t-\frac{k}{n-m}\right)(m+n). \tag{5}$$

Eq. (3) shows that the filtered harmonic wavelets attain non zero values in the frequency band [m2π, n2π]. Their centre frequency is (m+ n)π and their bandwidth is (n-m)2π, while symmetry is preserved making the transition from scale to frequency domain an easy task. Mathematically the filtered harmonic wavelets have an infinite support in the time domain as Eqs. (4) and (5) show, but the fairly fast decay that they exhibit, leads

to the definition of an effective support, so that the function is assumed to have a finite energy whose concentration depends on (n- m), besides k. The Hanning window function applied in the frequency domain for the filtered wavelets results in a narrower effective support in the time domain, improving their resolution in time over the generalized wavelets. However, contrary to the generalized harmonic wavelets that feature box-like spectra, the filtered wavelet transform does not define an orthogonal transform. Fortunately, if signal reconstruction is not an issue, as in the case of analyzing time-history records, this does not constitute a major drawback.

An important point concerning the practical implementation of the HWT is that the term 1/(n-m) determines the scale of harmonic wavelets and thus may be construed as the substitute of the scale parameter α. As it will be shown in the numerical results to be discussed in a forthcoming section of the paper, careful selection of the n, m parameters which is typically a case-dependent procedure may lead to a satisfactory balance between time and frequency resolution.

The complex harmonic wavelet coefficients of a function $f(t)$ satisfying Eq. (1) are given by the equation

$$w_{(m,n),k}(t) = (n-m)\int_{-\infty}^{+\infty} f(t)\psi^{*}_{(m,n),k}(t)dt\,. \tag{6}$$

From a computational point of view, it must be noted that the HWT utilizes the fast Fourier transform (FFT) which offers a significant advantage in terms of the requisite computational effort when long sequences are considered. This is achieved by performing the convolution that Eq. (6) describes for the corresponding discrete or sampled quantities in the frequency domain, where it becomes a simple multiplication (Newland,

1999). Taking into account the fact that the harmonic wavelets are conveniently defined in the frequency domain as in Eq.(3), the FFT algorithm need only to be applied to the function $f(t)$, and then the inverse FFT is used to obtain the wavelet coefficients in the time domain.

In analogy to standard time- frequency analysis procedures (Cohen, 1995), *the wavelet spectrogram* can be defined as

$$SP(t,\omega) = \left| w_{(m,n),k} \right|^2 . \tag{7}$$

Clearly, Eq. (7) yields a 3-D graphical direct representation of $f(t)$ versus time and frequency and constitutes the basic result for all the ensuing analyses of the accelerogram and the structural response records. Treating the wavelet spectrogram as a joint time-frequency density function the mean instantaneous frequency (Boashash, 1992a; Boashash, 1992b; Cohen, 1995) can be computed by the expression

$$MIF(t) = \frac{\int_{\omega} \omega SP(t,\omega) d\omega}{\int_{\omega} SP(t,\omega) d\omega} . \tag{8}$$

Strictly speaking, Eq. (8) averages the wavelet spectrogram over all frequencies considered at a specific time instant and normalizes the outcome over the whole spectrum. Intuitively, it gives the temporal change of the mean value of the frequencies contained in the signal. Clearly, the averaging procedure eliminates local fluctuation and thus can yield more readily discernible information about the temporal evolution of the frequency content of a particular signal.

3. Historic accelerograms and the benchmark structural system description

Four historic earthquake records are studied to illustrate the appropriateness of the harmonic wavelet transform to provide information about the time-frequency characteristics of ground acceleration records pertaining to major earthquake events. The El Centro (N-S component recorded at the Imperial Valley Irrigation District substation in El Centro, California, during the Imperial Valley, California earthquake of May 18, 1940), and the Hachinohe (N-S component recorded at Hachinohe City during the Takochi-oki earthquake of May 16, 1968), earthquakes have been selected as far-field examples. The Northridge (N-S component recorded at Sylmar County Hospital parking lot in Sylmar, California, during the Northridge, California earthquake of January 17, 1994), and the Kobe (N-S component recorded at the Kobe Japanese Meteorological Agency (JMA) station during the Hyogo-ken Nanbu earthquake of January 17, 1995), earthquakes have been chosen as near-field examples. This selection of historic data is motivated by the fact that they have also been used in benchmark studies related to structural control (Ohtori et al., 2004). Figure (1) shows the accelerograms of these strong ground motions.

The usefulness of the harmonic wavelet transform for capturing localized frequency content is further investigated in this study by considering the nonlinear structural seismic responses of a particular structure. To this end, the nonlinear dynamic response of a benchmark 20-story steel frame introduced in Spencer et al. (1999) and Ohtori et al. (2004), to the preceding accelerograms is derived. It was designed by Brandow & Johnston Associates for the SAC Phase II Steel Project and is part of a

typical mid- to high-rise building which meets the seismic code for the Los Angeles, California region.

The structural system consists of moment- resisting frames (MRFs), at the perimeter to engage lateral loads, and simple framing in the interior. The columns are 345 MPa steel and the floors are composite with 248 MPa steel beams and concrete. The model of the building along with information regarding various structural parameters is shown in Figure (2). The floors are assumed to be rigid in the horizontal plane and thus diaphragmatic action holds. The inertia forces are assumed to be evenly distributed on the two moment resistant frames. Symmetry allows an in-plane 2-D analysis of half of the entire building and thus only one MRF along the weak N-S direction is considered. The mathematic model described in Spencer et al. (1999), is adopted for the boundary conditions and the discretization of the elastic and inertia properties of the frame. The first five natural frequencies of the frame are 0.261, 0.753, 1.30, 1.83 and 2.40 Hz. A trilinear hysteresis model for structural member bending, as the one shown in Figure (3), is used.

4. Numerical results/ Joint time-frequency spectra

4.1 Accelerograms

The wavelet transform has been employed to analyze the four aforementioned accelerograms using the filtered harmonic wavelets. Certain plots summarizing the numerical results obtained are shown in figures (4), (5), (6) and (7), corresponding to the El Centro, Hachinohe, Northridge and Kobe earthquake records, respectively. In the (a) plot of each figure the percentage of the total energy of the signal that is captured at different frequencies is given, resulting from standard Fourier transform analysis.

The (b) plots present the 3-D wavelet spectrograms as computed by Eq. (7). It is noted that although three indices appear in the local spectrum notation, two relate to frequency (m, n), and the third defines the time position (k). Thus, by changing the values of m and n one may have a trade-off between time and frequency resolution in the general harmonic wavelet map, where the uncertainty principle applies. After several trials, the difference n-m= 10 is found to yield a meaningful compromise between time and frequency resolution.

A comparison of the above plots for each record shows clearly the advantages of a joint time-frequency analysis for earthquake accelerograms. Not only does it offer a useful representation of the overall frequency content of the signal, just like the standard Fourier analysis does, but it also succeeds to capture the evolution of the frequencies present in time for as long as the earthquake lasts. Moreover, note the smoothness of the wavelet spectrograms and the resolution by which the filtered harmonic wavelets represent the signals at all frequency bands that are of interest.

Contour plots of the wavelet spectrograms are provided in the (c) part of the figures where the mean instantaneous frequency (MIF), as computed by Eq. (8), is superimposed; the time histories of the accelerograms (d) are shown as well to expedite the physical interpretation. In this manner, a more efficient joint time- frequency representation is achieved from a practical point of view, and the evolution in time of the frequency content of the signal becomes even more apparent.

Examining these numerical results, expected trends due to the characteristics of the recorded events are clearly captured by the analysis. In general, the higher frequencies are more dominant during the “growth phase” of the accelerograms and then

decay following a rate that is influenced by many parameters whose consideration is beyond the scope of the present paper.

4.2 Structural response

The joint time-frequency analysis using the harmonic wavelet transform was next implemented to extend early works such as that of Roesset (1986), to capture the influence of nonlinearity on the variation of the effective natural frequencies of yielding structural systems during the evolution of a seismic event, and to demonstrate the potential of the method for damage detection purposes. In particular, the inelastic structural response of the 20- story steel frame of Figure (2) has been determined for various amplitude levels of excitation using as input the four previously analyzed ground accelerations of Figure (1). The standard β-Newmark algorithm with the assumption of constant acceleration at each time step (values $\beta=1/4$, $\gamma=1/2$), was implemented for the purpose of accounting for the non linear behavior of the frame under consideration, as extensively described in Ohtori et al. (2004).

The harmonic wavelet transform was applied to the lateral displacement response of the first floor. To assess the effectiveness of the harmonic wavelets as an analytical damage detection tool two extreme cases are considered in Figures (8) and (9) where the plots included are of the same kind and order as discussed before. In Figure (8), the El Centro accelerogram scaled by the factor 0.5 is used as input, so that the frame stays in the elastic region, whereas for the El Centro accelerogram scaled by 2.50 (Figure (9)) the frame suffers structural damage witnessed by permanent deformations. For reference purposes the first five natural frequencies of the elastic frame are shown on the plots.

In this context, it is noted that linear structural systems exhibit highly resonant transfer functions and thus act like pass-band filters to earthquake signal inputs yielding output- response signals characterized by the structural natural frequencies. Further, when they are forced to exhibit inelastic behavior their effective natural frequencies decrease, due to stiffness degradation. Both trends can be readily seen in Figures (8) and (9) in the traditional Fourier spectrum plots (a), and the wavelet spectrograms (b), (c). Obviously, the joint time- frequency representation gives additional time localization information about the effective frequencies of the response signals and adequately captures their evolution in time.

More importantly, in this case the MIF can be construed as a structural damage indicator. Clearly, the structural response signal in the frequency domain is determined as the product of the transfer function of the structure times the Fourier transform of the input signal. For any particular effective temporal segment, the MIF of the response averages this product over the frequency domain. Note that the MIF of the El Centro accelerogram oscillates around a mean value of roughly 3Hz as seen in Figure (4c), while the first two natural frequencies of the elastic structure attain much lower values of 0.26Hz and 0.75Hz. During the first few seconds of both of the response signals examined in Figures (8c) and (9c) the MIF practically remains the same. Primarily, the elastic transfer function is involved in the averaging, since the input signal has not been substantially build up, yet. During the period which follows up to the 30^{th} second when most of the energy of the strong ground motion has been induced to the structure, the MIF decreases in both cases. It is clear that in this case the MIF averages the product of the effective transfer function of the structure with the spectrum of the excitation. In the

case of the scaled by 2.5 input, there is an expected overall trend of the MIF curve towards the lower frequencies when compared to the response induced by the input scaled by 0.5. After the 30th second, which roughly marks the effective duration of this particular strong ground motion, the structural response becomes primarily free vibration response. Thus, in the elastic case, the MIF converges to its value corresponding to the beginning of the seismic event, since, of course, the dynamic characteristics of the structure, remain the same. On the contrary, for the 2.50 El Centro input, the MIF value remains in much lower levels as the frame has undergone plastic deformations. In the Fourier spectrum (Figure 9b), this is manifested by a dominant dc component, which is entirely absent from the Fourier spectrum of the elastic case response. Evidently, this new "mode" contributes significantly to the drop in MIF for the 2.5 El Centro input after the 30th second of the signal.

5) Concluding remarks

The present article has extended earlier efforts made in Spanos et al. (2005), regarding applications of wavelets on various nonstationary signals frequently encountered in earthquake and structural engineering, in general.

In this regard, the harmonic wavelet transform, incorporating the enhanced time resolution and the appealing properties in frequency domain of the filtered harmonic wavelets, has been employed to analyze historic earthquake accelerograms and time histories of inelastic structural response to seismic signal inputs. Signals of this nature are inherently non stationary as their intensity and frequency content varies with time and thus call for a joint time- frequency representation.

In this context, four ground acceleration records pertaining to two near-field and two far- field major earthquake events have been analyzed via this signal processing tool, and smooth 3-D wavelet spectrograms have been obtained with strong resolution at all frequency bands that are of interest. Certain observations have been made regarding the numerical results and the appropriateness of the time-frequency representation for capturing the evolving frequency content vis a vis the traditional Fourier amplitude spectrum.

Furthermore, the harmonic wavelet transform has been applied to the lateral displacement response of the first floor of a 20-story steel frame exposed to one of the four historical accelerograms scaled by appropriate factors to simulate undamaged and severely damaged conditions for the structure. The effectiveness of the harmonic wavelet transform as a detection tool for global structural damage has been demonstrated. In this context, attention has also been focused on the usefulness of the mean instantaneous frequency. The latter decreases significantly when the frame is forced to exhibit inelastic behavior, reflecting the overall reduction of the effective natural frequencies due to stiffness degradation and health deterioration of structure.

It is believed that studies such as the present will further familiarize the structural engineering community with the advantages of custom-made joint time- frequency analyses and will establish wavelets and other related concepts as indispensable tools of modern signal localization capturing and system/ structure health monitoring.

6) Acknowledgements

The financial support of this work by a grant from NSF is greatly acknowledged.

References

Boashash, B. (1992a), Estimating and interpreting the instantaneous frequency of a signal. I. Fundamentals, in *Proceedings of the IEEE*, **80**(4), 520-538.

Boashash, B. (1992b), Estimating and interpreting the instantaneous frequency of a signal. II. Algorithms and applications, in *Proceedings of the IEEE*, **80**(4): 540-568.

Burrus, C.S. Gopinath, R.A. Guo, H. (1997), *Introduction to Wavelets and Wavelet Transforms- A Primer,* Upper Saddle, River, Prentice- Hall, New Jersey.

Cohen, L. (1995), *Time- Frequency Analysis*, Prentice- Hall PTR, New Jersey.

Haigh, S.K. Teymur, B. Madabhushi, S.P.G. & Newland, D.E. (2002), Applications of wavelet analysis to the investigation of the dynamic behavior of geotechnical structures, *Soil Dynamics and Earthquake Engineering*, **22**, 995-1005.

Hou, Z., Noori, M. & Amand, R., St. (2000), Wavelet–based approach for structural damage detection." *Journal of Engineering Mechanics,***126**(7), 677-683.

Kim, D.S. & Park, H.C. (2002), Determination of dispersive phase velocities for SASW method using harmonic wavelet transform, *Soil Dynamics and Earthquake Engineering*, **22**(8), 675-684.

Mallat, S. (1998), *A Wavelet Tour of Signal Processing*, Academic Press, London.

Newland, D.E. (1994a), Wavelet analysis of vibration, part I: Theory, *Journal of Vibrations and Acoustics*, **116**, 409-416.

Newland, D.E. (1994b), Wavelet analysis of vibration, part II: Wavelet maps, *Journal of Vibrations and Acoustics*, **116**, 417-425.

Newland, D.E. (1997), Practical signal analysis: do wavelets make any difference?, in: *Proceedings of the 1997 ASME Design Engineering Technical Conferences, 16th*

Biennial Conference on Vibration and Noise, Paper DETC97/VIB-4135 (CD ROM ISBN 07918 1243 X), Sacramento, California.

Newland, D.E. (1999), Ridge and phase identification in the frequency analysis of transient signals by harmonic wavelets, *Journal of Vibrations and Acoustics*, **121**, 149-155.

Newland, D.E. & Butler, G.D. (2000), Application of time- frequency analysis to transient data from centrifuge earthquake testing, *Shock and Vibration*, **7**, 95-202.

Ohtori, Y. Christenson, R.E. Spencer, B.F.J. & Dyke, S.J. (2004), Benchmark structural control problems for seismically excited nonlinear buildings, *Journal of Engineering Mechanics*, **130**: 366-385.

Qang, Q. & Deng, X. (1999), Damage detection with spatial wavelets, *International Journal of Solids and Structures* **36**, 3443-3468.

Roesset, J.M. (1986), Nonlinear dynamic response of frames, In: *8th Symposium on Earthquake Engineering*, Roorkee, **1**, 435-442.

Spanos, P.D. & Failla, G. (2004), Evolutionary spectra estimation using wavelets, *Journal of Engineering Mechanics*, **130**, 952- 960.

Spanos, P.D. & Failla, G. (2005), Wavelets: Theoretical concepts and vibrations related applications, *The Shock and Vibration Digest*, **37**(5), 359-375.

Spanos, P.D. Tezcan, J. & Tratskas, P. (2005), Stochastic processes evolutionary spectrum estimation via harmonic wavelets. *Computer Methods in Applied Mechanics and Engineering*, **194**, 1367-1383.

Spanos, P.D. Failla, G. Santini, A. & Pappatico, M. (2006), Damage detection in Euler-Bernoulli beams via spatial wavelet analysis, *Structural Control and Health Monitoring,* **13**, 472-487.

Spencer, B.F.J. Christenson, R.E. Dyke, S.J. (1999), Next generation benchmark control problems for seismically excited buildings, in Kobori, T., et al, Ed., *Proceedings of the 2nd World Conference on Structural Control*, Wiley, New York, **2**, 1135–1360.

Zhou, Z. & Adeli, H. (2003a), Time-frequency signal analysis of earthquake records using Mexican hat wavelets, *Computer-Aided Civil and Infrastructure Engineering*, **18**(5), 379-389.

Zhou, Z. & Adeli, H. (2003b), Wavelet Energy Spectrum for Time-Frequency Localization of Earthquake Energy, *International Journal of Imaging Systems and Technology*, **13**(2), 133-140.

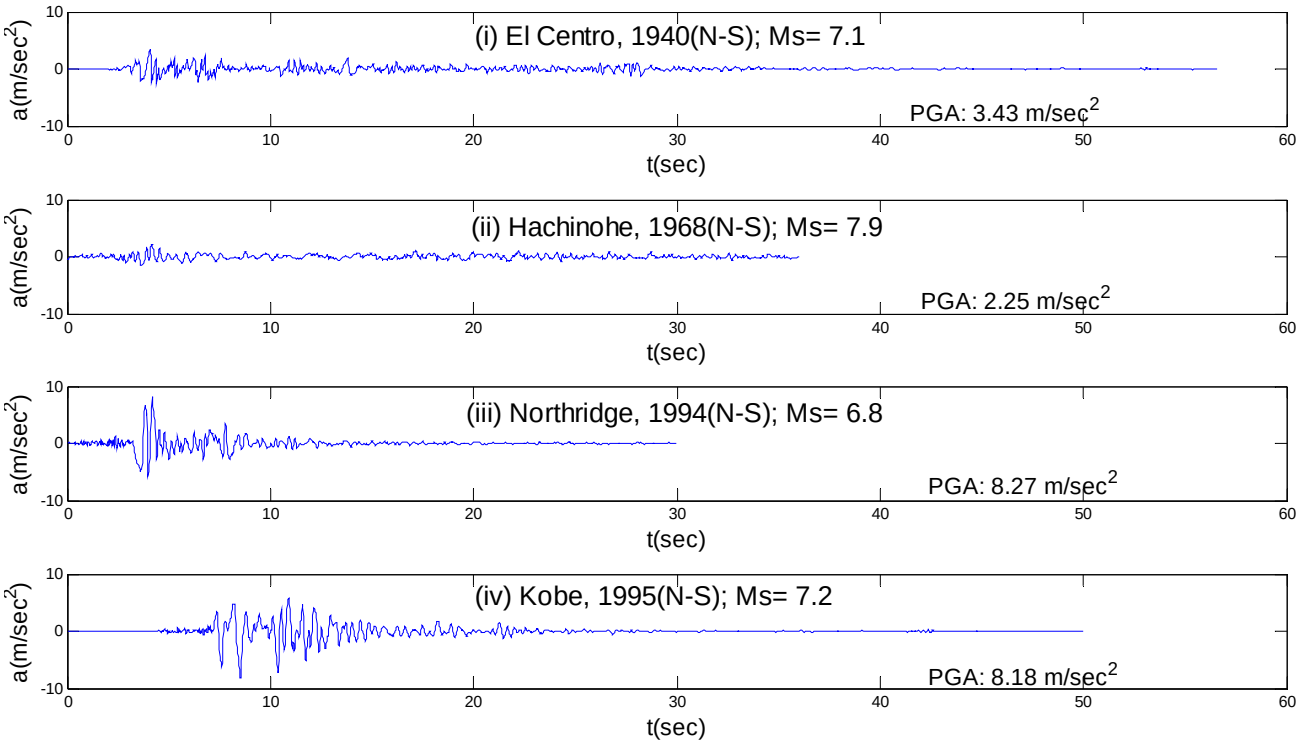

Figure (1): Earthquake accelerograms considered.

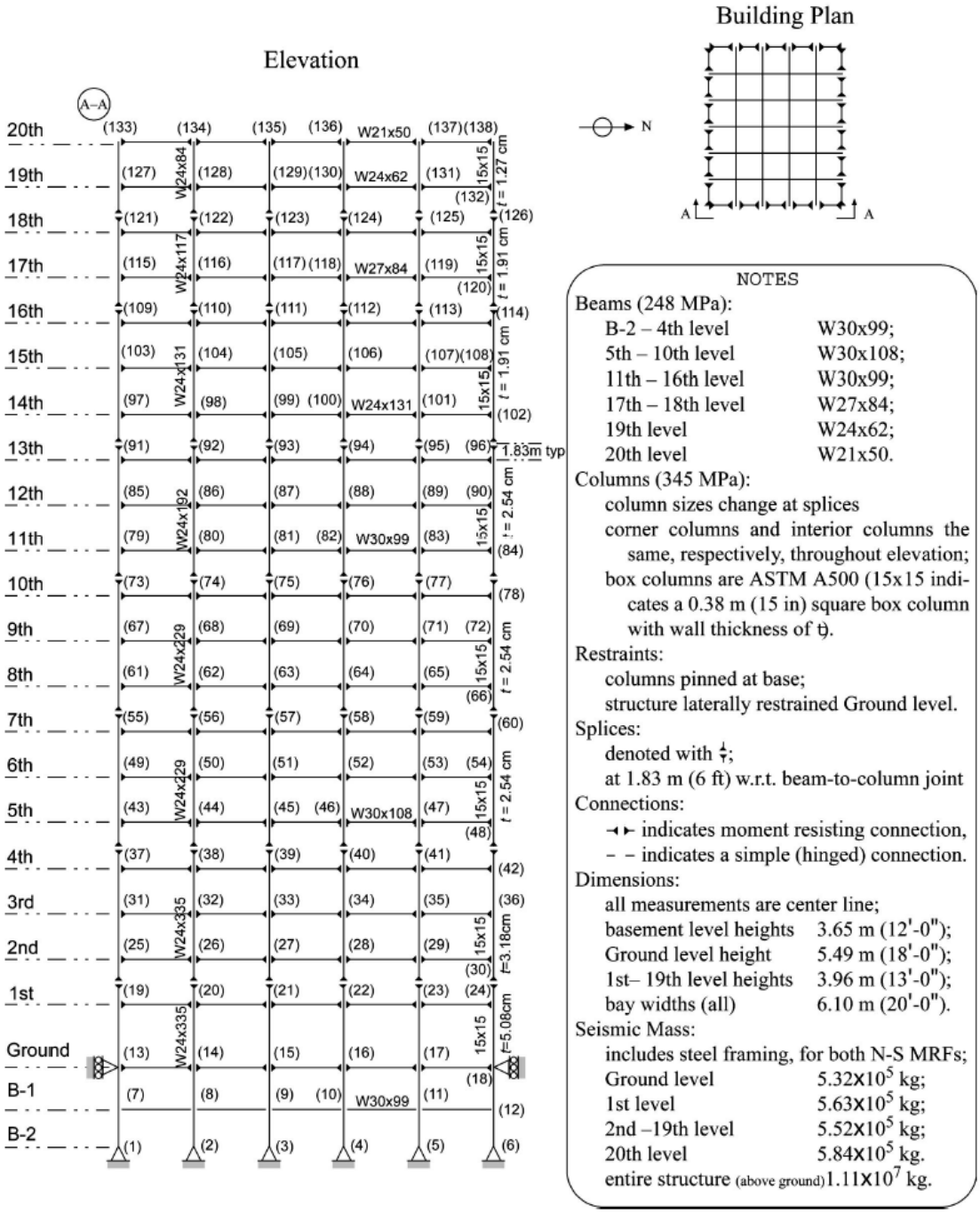

Figure (2): Benchmark 20-story steel frame used in the analysis of typical mid- to high-rise building's response to earthquake excitations (after Spencer et al. 1999).

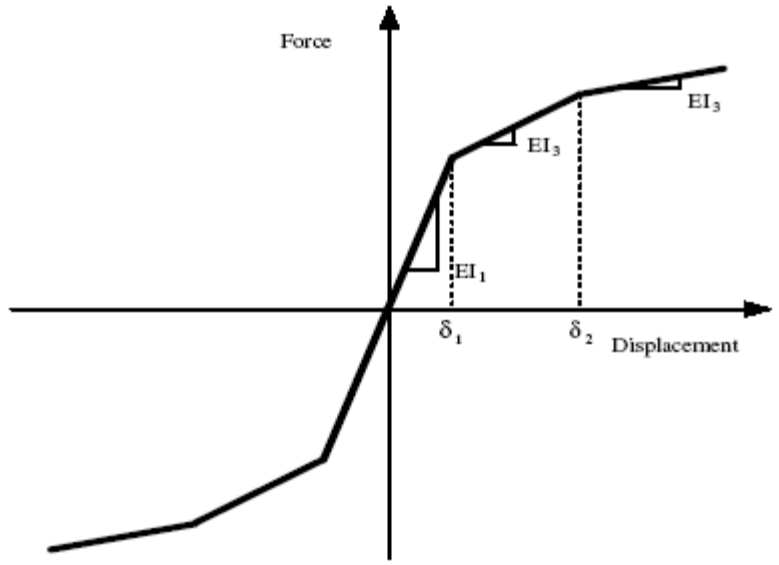

Figure (3): Trilinear hysteresis model for structural member bending.

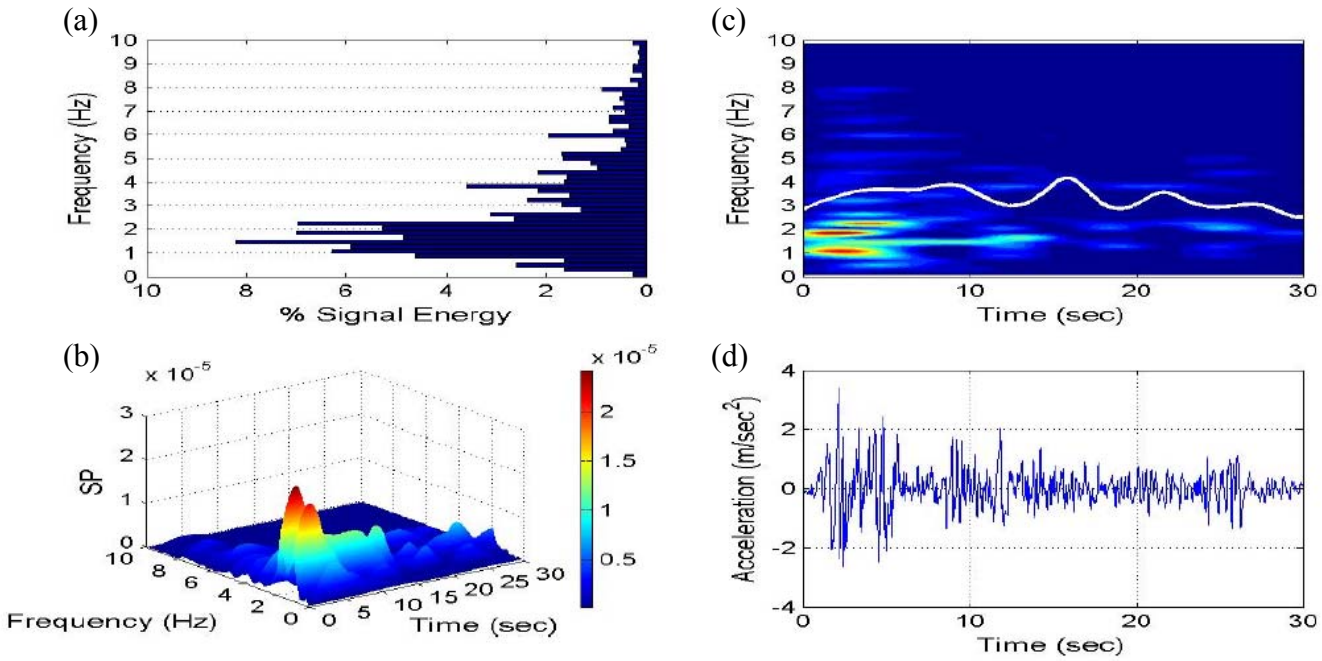

Figure (4): Joint time-frequency analysis of the El Centro N-S component earthquake via harmonic wavelet transform

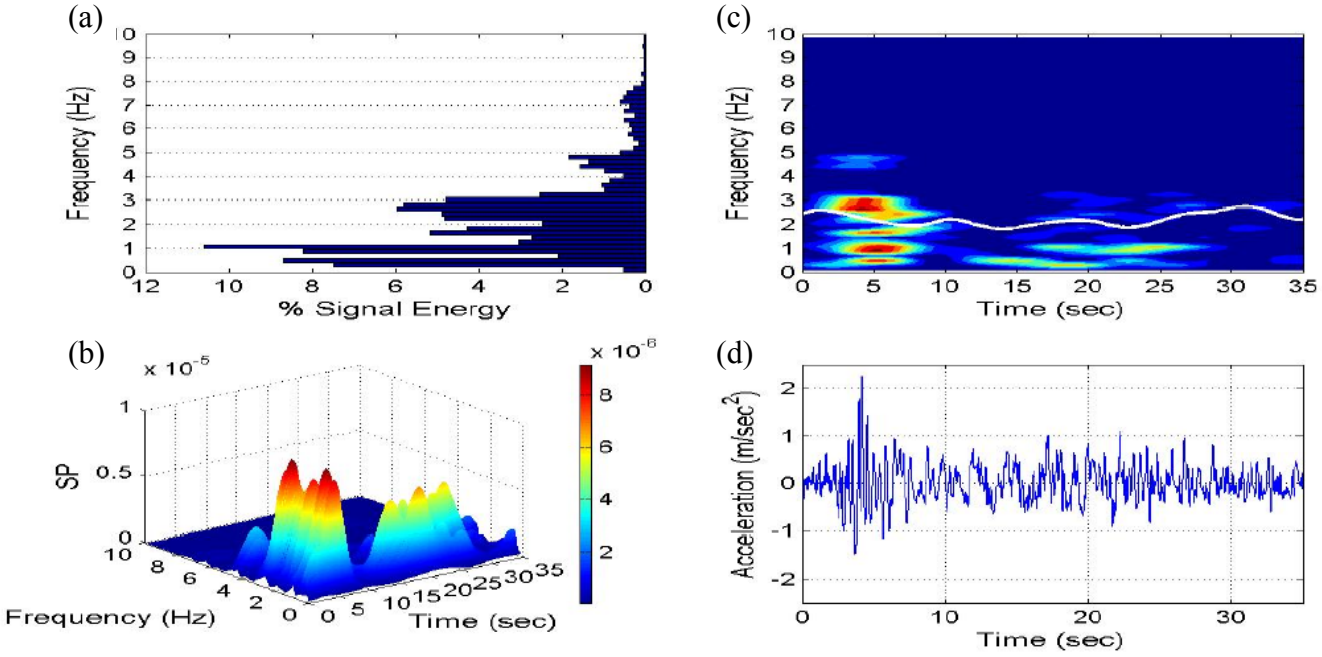

Figure (5): Joint time-frequency analysis of the Hachinohe N-S component earthquake via harmonic wavelet transform

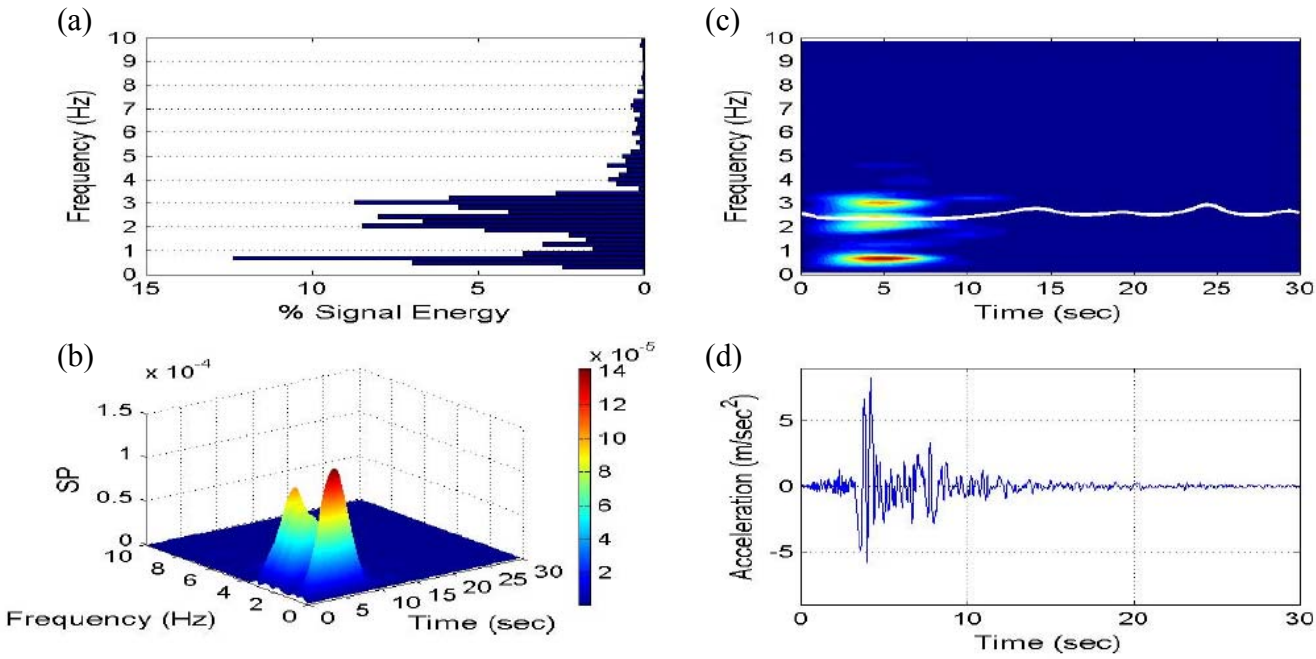

Figure (6): Joint time-frequency analysis of the Northridge N-S (Sylmar) component earthquake via harmonic wavelet transform

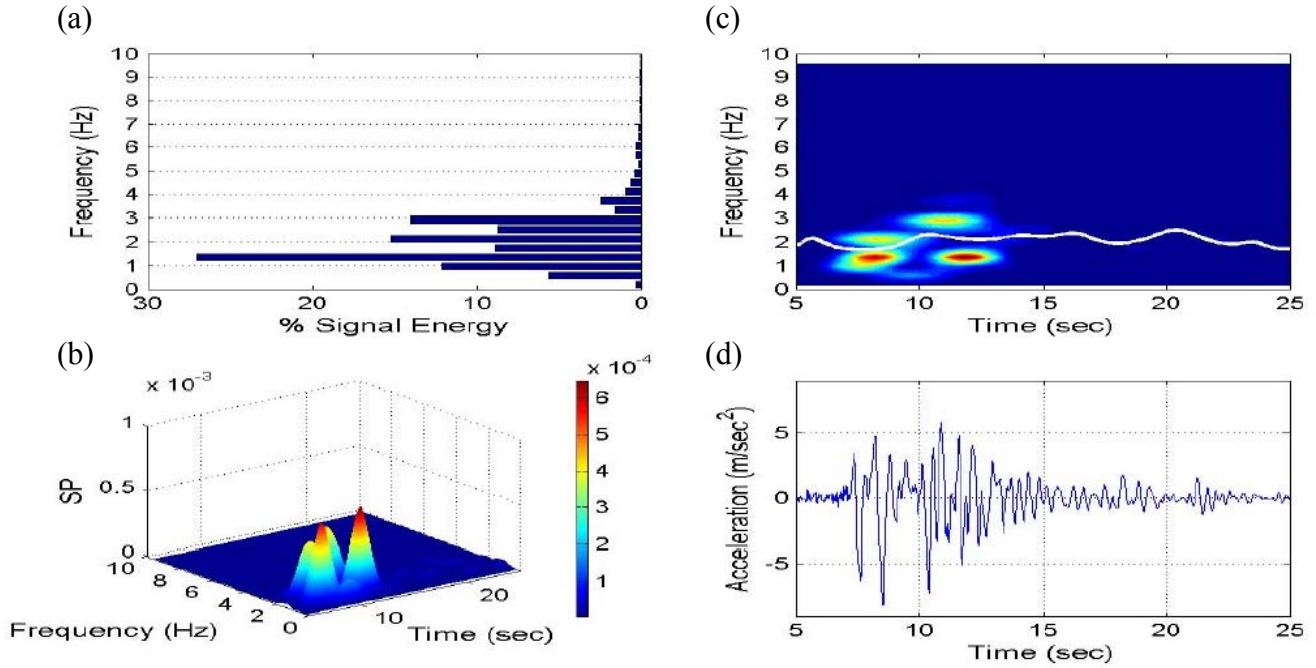

Figure (7): Joint time-frequency analysis of the Kobe N-S component earthquake via harmonic wavelet transform

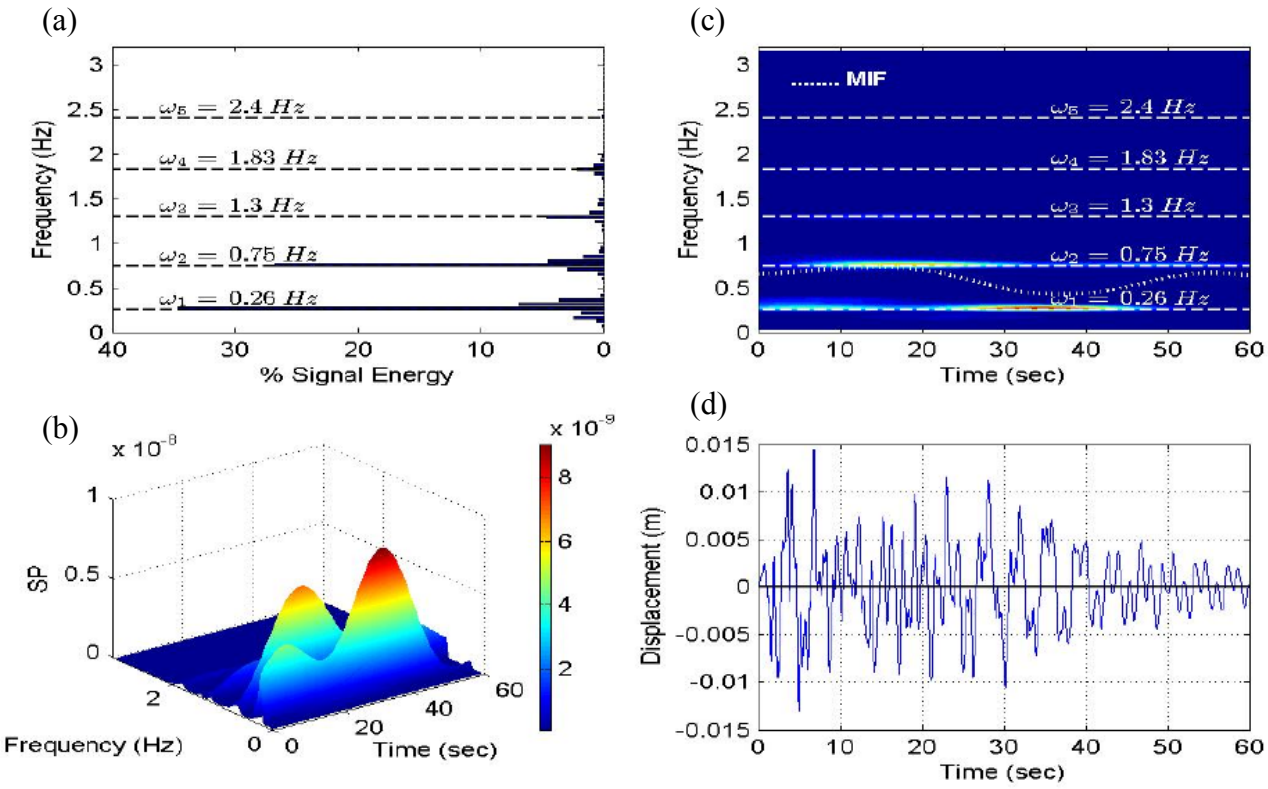

Figure (8): Joint time-frequency analysis of the first floor lateral displacement response to 0.50·El Centro ground acceleration input.

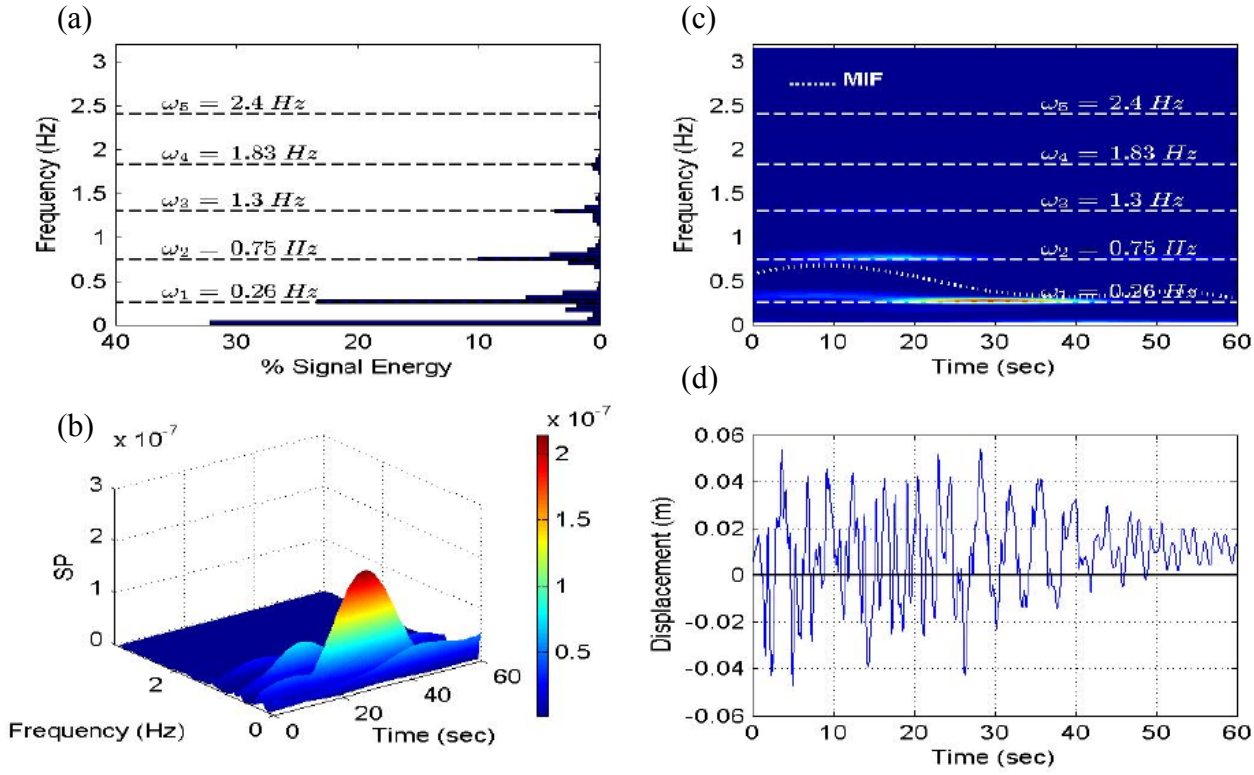

Figure (9): Joint time-frequency analysis of the first floor lateral displacement response to 2.50·El Centro ground acceleration input.